Shock waves in superfluid helium

D. M. Moody and B. Sturtevant
Graduate Aeronautical Laboratories, California Institute of Technology, Pasadena, California 91125

(Received 15 September 1983; accepted 10 February 1984)

Exact solutions of the equations of motion of liquid helium II can be compared to experiments to test Landau's two-fluid theory. The best flows with which to conduct such tests are those in which amplitudes and gradients are large and in which the calculations and measurements are free from wall effects, e.g., shock waves. The four fundamental conservation equations of superfluid mechanics have been integrated across a one-dimensional discontinuity (shock wave) propagating into undisturbed helium II to yield a set of four algebraic equations (jump conditions) which, when supplemented by thermodynamic state information, establish the equilibrium flow state behind the shock wave for a given wave speed and undisturbed flow state ahead of the shock. These jump conditions have been solved numerically for 19 points on the helium II p-T diagram with upstream Mach number as the independent parameter. Representative results of the calculations are presented for pressure shocks, temperature raising shocks, and temperature lowering shocks. The results are compared to previous analytical approximate solutions to test the validity of those approximations. They are also compared to experimental data for shock waves in helium II as a means of testing the correctness of the full nonlinear two-fluid equations.

I. INTRODUCTION

This work was undertaken as an attempt to shed light upon the implications of data from experiments on shock waves in superfluid helium. The data provide a means of testing the correctness of the nonlinear two-fluid model if the shock jump conditions which follow from this model can be solved. The two-fluid theory of superfluid helium (or helium II) consists of two rather distinct parts: a fluid dynamic formulation given by a set of conservation equations from which the shock jump conditions are obtained, and a thermodynamic description in the form of state equations which interrelate state variables appearing in the jump conditions. The complexity of these equations precludes closed form, analytical solutions, and only linearized approximations for weak shocks have heretofore been obtained. The experimental shock wave data in some cases show significant disagreement with these approximations, and an important question then arises. Are the disagreements a consequence of the weak wave approximation; or, more fundamentally, do they indicate a failure of the two-fluid model? Our objective here is to eliminate the former possibility by solving the superfluid jump conditions numerically.

We incorporate into our shock solutions the thermodynamics of helium II given by Maynard.[1] His experiments and calculations provide pressure and temperature dependences of the state variables to a precision of about 0.3%. Dependence on the counterflow velocity is approximated to leading order by neglecting the w dependence of the normal fluid fraction. The effect of this approximation on our solutions is discussed.

The dynamics of helium II is described by four conservation equations for mass, momentum, energy, and superfluid motion (see, for example, Landau and Lifshitz[2] or Putterman[3]). The conservation equation of superfluid motion preserves irrotationality in the superfluid velocity field. In nondissipative flows, i.e., those in which the products of gradients with transport coefficients are negligible, entropy is also conserved. In these cases, the entropy conservation equation is equivalent to energy conservation and thus does not overspecify the flow field. In flows with high gradients, e.g., flows through shock waves, entropy is not conserved, and Khalatnikov[4] has extended the hydrodynamics of helium II to include dissipation and thus detail how entropy is produced in such cases. Although shock waves, with their large temperature and velocity gradients, produce entropy, these gradients have no effect on an integral balance of mass, momentum, and energy across the discontinuity. Whether or not superfluid motion is conserved (i.e., whether or not the superfluid velocity field remains curl-free) through shock waves in helium II is more controversial. In a recent paper, Atkin and Fox[5] compare the results of experiment with weak wave theory for pure temperature shocks (cf. Sec. I B) to determine whether entropy or superfluid motion is conserved in addition to mass, momentum, and energy. They find a slight preference for entropy conservation. In this paper, following Khalatnikov,[4,6] we have taken the more conventional approach and have allowed for entropy generation.[7] The jump conditions are solved exactly (without second-order expansions and without neglect of mode coupling) for superfluid shocks propagating into quiescent liquid, and the results are then compared to experiment. It should be noted that the experiments and calculations presented here are tests of the shock jump conditions and do not address the effects of nonuniform downstream flow and shock decay.

Early experiments[8,9] on temperature shocks in helium II confirmed the nonlinear behavior of large-amplitude second sound. In this laboratory, a series of experiments has been carried out by Cummings[10] (cf. also Cummings *et al.*[11]), Wise,[12] Turner,[13,14] and Torczynski.[15] We compare the results of the present investigation with results from Wise and

 0031-9171/84/051125-13$01.90

Torczynski. Preliminary numerical results were reported by Sturtevant.[16]

Comparison of the present results to pressure shock data shows good agreement for experiments at temperatures below 1.88 K. Disagreements above 1.88 K are probably due to evaporative effects. Comparison to temperature shock data shows agreement for low Mach numbers but significant disagreement at higher Mach numbers. The higher Mach number temperature shock data might be used to improve the two-fluid thermodynamics. However, it is possible that these data are not simply indicative of the approximate nature of the thermodynamic relations used; they may also indicate inaccuracy of the two-fluid conservation equations.

A. The two-fluid model and thermodynamics of helium II

At temperatures below 2.17 K on its saturated vapor pressure curve, ^{4}He exists as a superfluid liquid phase called helium II. Many of the peculiar behaviors of this phase have been successfully explained by a macroscopic hydrodynamic and thermodynamic model put forth by Landau and others (see, for example, Refs. 2 and 3). This so-called two-fluid model assumes that helium II consists of two components. One, called the supercomponent, is imagined to be a perfect liquid, while the other, called the normal component, is assumed to carry all of the fluid's entropy and to be responsible for viscous interactions. Each component is assigned its own density and velocity fields. The total fluid density $\tilde{\rho}$ is given by the sum of the super and normal component densities;

$$\tilde{\rho} = \rho_s + \rho_n . \tag{1}$$

The relative velocity $\mathbf{w}$ between the two components (also called the counterflow velocity) is defined as

$$\mathbf{w} = \mathbf{u}_n - \mathbf{u}_s , \tag{2}$$

while the ordinary flow velocity $\mathbf{u}$ is given by

$$\tilde{\rho}\mathbf{u} = \rho_s \mathbf{u}_s + \rho_n \mathbf{u}_n . \tag{3}$$

Because entropy (and thus heat) is convected with the normal component, the thermodynamic identity for the fluid must be extended;

$$d\tilde{\mu} = -\tilde{s}\, dT + (1/\tilde{\rho})dp - (\rho_n/\tilde{\rho})\mathbf{w}\cdot d\mathbf{w} . \tag{4}$$

Here, $\tilde{\mu}$ is the chemical potential per unit mass, $\tilde{s}$ the specific entropy, T the temperature, and p the pressure. It is the last term of the above equation which indicates reversible heat transport by the normal component, and it is this dependence of the thermodynamics on the dynamic quantity w^2 which complicates the solution of the equations of motion, but at the same time generates one of the greatest motivations for seeking solutions. If one assumes, for small counterflow velocities, that the normal fluid fraction $\rho_n/\tilde{\rho}$ is independent of w^2, Eq. (4) may be integrated to give

$$\tilde{\mu}(p,T,w^2) \approx \mu(p,T) - (w^2/2)(\rho_n/\rho) , \tag{5a}$$

where all quantities on the right-hand side are functions of p and T only. The tilde is used over state variables to emphasize dependence on the counterflow velocity. Entropy and density are then found by differentiating Eq. (5a) with respect to temperature and pressure;

$$\tilde{s}(p,T,w^2) \approx s(p,T) + \frac{w^2}{2}\frac{\partial}{\partial T}\left(\frac{\rho_n}{\rho}\right) , \tag{5b}$$

$$\tilde{\rho}(p,T,w^2) \approx \rho(p,T) + \frac{\rho^2 w^2}{2}\frac{\partial}{\partial p}\left(\frac{\rho_n}{\rho}\right) . \tag{5c}$$

For our shock jump calculations, we use the above state equations. Pressure and temperature dependences of all the thermodynamic quantities are taken from the work of Maynard.[1]

One may estimate an upper bound on the error which results from using in Eqs. (5) the approximate quadratic dependence on counterflow velocity. Using ideal Bose statistics, Khalatnikov[4] derives an expression for ρ_n as a function of temperature and counterflow velocity. According to his result, at $T = 1.609$ K, ρ_n is increased by only 1.2% above its static ($w = 0$) value when $w = 3.8$ m/sec, a value which is larger than any of the experimental counterflow velocities considered in this work. However, the predicted static value is almost 20% below that measured by Maynard,[1] which calls into question the validity of an ideal analysis at these temperatures. The dependence of ρ_n on w in vortex-free fourth sound is apparently beyond current experimental resolution.[17]

B. Shock waves in helium II and the jump conditions

Consider the quantities which specify an equilibrium (i.e., nondissipative) flow state in helium II. Upon inspection of Eq. (4) it is clear that pressure, temperature, and magnitude of counterflow velocity may be chosen as the independent variables necessary to thermodynamically specify the state. Dynamically, the vectors $\mathbf{u}$ and $\mathbf{w}$ (or equivalently $\mathbf{u}_n$ and $\mathbf{u}_s$) are required. Therefore, two vector equations (conservation of momentum and superfluid motion) and two scalar equations (conservation of mass and energy) are necessary in the two-fluid model.

It is well known that linearization of these conservation equations yields two uncoupled linear wave modes in the approximation of zero thermal expansion. These modes describe the propagation of small-amplitude disturbances in helium II. One is the familiar sound wave (called first sound in helium II) which propagates pressure-density disturbances at a speed given by

$$a_1 = \left(\frac{\partial p}{\partial \rho}\right)_s^{1/2} , \tag{6}$$

while the other mode (called second sound) is unique to helium II and propagates temperature-entropy disturbances as waves at a speed given by

$$a_2 = (\rho_s s^2 T/\rho_n c_p)^{1/2} . \tag{7}$$

For large-amplitude disturbances, the nonlinear terms in the dynamic and thermodynamic equations provide for the occurrence of wave steepening and ultimately shock wave formation. The jump in flow state across the shock is deduced by integrating the conservation equations of mass, momentum, energy, and superfluid motion across the discontinuity (shock wave). The integration is effected in the usual manner by transforming to a steady coordinate system. Consider a one-dimensional shock wave propagating into undisturbed helium II with speed c (see Fig. 1), and from

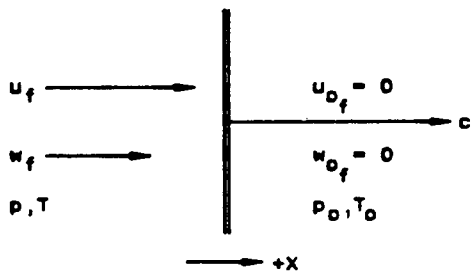

FIG. 1. Lab-fixed coordinates.

this lab-fixed coordinate system (denoted by f) transform to a system in which the shock is fixed (Fig. 2). The zero subscript refers to unshocked fluid. Note that the relative velocity w is invariant under this transformation, and as a result, a conventionally positive relative velocity in lab-fixed coordinates (i.e., toward the shock) will be negative in the shock-fixed frame. The flow is steady in the shock-fixed frame; thus the fluxes of mass, momentum, superfluid motion, and energy must match across the shock (see Khalatnikov[4,6]),

$$\tilde{\rho}u = \rho_0 u_0 , \tag{8}$$

$$p + \tilde{\rho}u^2 + (\rho_s\rho_n/\tilde{\rho})w^2 = p_0 + \rho_0 u_0^2 , \tag{9}$$

$$\tilde{\mu} + \tfrac{1}{2}u_s^2 = \mu_0 + \tfrac{1}{2}u_{s_0}^2 , \tag{10}$$

$$\tilde{\rho}\tilde{s}Tu_n + \rho_n u_n^2 w = \rho_0 s_0 T_0 u_{n_0} . \tag{11}$$

The above four equations are the superfluid (i.e., helium II) shock jump conditions, and one can note that they reduce to their counterparts for a classical fluid when $w = 0$. It is helpful to rearrange the set in nondimensional form. Upon eliminating u_n and u_s in favor of u and w, and then eliminating u by Eq. (8), we may write

$$f_1 = \frac{p - p_0}{\rho_0 a_0^2} + \left(\frac{\rho_0}{\tilde{\rho}} - 1\right)M^2 + \frac{\rho_s\rho_n w^2}{\rho_0\tilde{\rho}a_0^2} = 0 , \tag{12}$$

$$f_2 = \frac{\tilde{\mu} - \mu_0}{a_0^2} + \frac{1}{2a_0^2}\left(\frac{\rho_0}{\tilde{\rho}}a_0 M - \frac{\rho_n}{\tilde{\rho}}w\right)^2 - \frac{1}{2}M^2 = 0 , \tag{13}$$

$$f_3 = \left(\frac{\tilde{s}T}{s_0 T_0} - 1\right)M + \frac{\rho_s\tilde{s}Tw}{\rho_0 s_0 T_0 a_0} + \frac{\rho_n w}{\rho_0 s_0 T_0 a_0}\left(\frac{\rho_0}{\tilde{\rho}}a_0 M + \frac{\rho_s}{\tilde{\rho}}w\right)^2 = 0 . \tag{14}$$

The wave speed $c = u_0$ has been expressed as the product of a shock Mach number M and a generic upstream sound speed a_0. It is generic because shock waves in helium II are of two types which correspond to the linear wave modes of first and second sound in the limit of vanishingly small wave strengths. Thus the Mach number for a pressure (or first sound) shock which primarily jumps the pressure, density, and total flow velocity u is based on first sound speed a_1, while the Mach number for a temperature (or second sound) shock which primarily jumps the temperature, entropy, and counterflow velocity w is based on the second sound speed a_2. For a given upstream thermodynamic state (specified by p_0 and T_0) and a given wave speed $c = Ma_0$, the three jump conditions [Eqs. (12)–(14)], supplemented by state equations for $\tilde{\mu}$, $\tilde{s}$, $\tilde{\rho}$, and $\rho_n/\tilde{\rho}$, specify the downstream state p, T, and w.

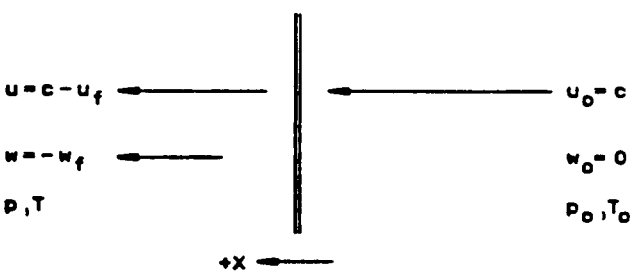

FIG. 2. Shock-fixed coordinates.

II. SOLUTIONS OF THE JUMP CONDITIONS

A. The Khalatnikov approximations

As mentioned previously, whether or not the experimental shock wave data confirm the validity of Landau's equations requires comparison to solutions of the jump conditions which follow from those equations. The solutions against which authors have traditionally compared their results are actually approximations made by Khalatnikov[4,6] to the exact solutions. These solutions are approximate in the sense that weak shock waves (i.e., $M = 1 + \epsilon$; $\epsilon \ll 1$) are considered, in which case the jumps in all quantities across the shocks are small. Jumps in temperature $\Delta T = T - T_0$, pressure $\Delta p = p - p_0$, and counterflow velocity w are chosen as the independent variables and each one is considered $O(\epsilon)$. Then all quantities which appear in the jump conditions are expanded as Taylor series in these variables, and only terms through $O(\epsilon^2)$ are retained. As a further approximation, the coefficient of thermal expansion is neglected. The results for pressure shocks are

$$\Delta p = 2(M-1)\left(\frac{\partial}{\partial p}\ln(\rho a_1)\right)_0^{-1} , \tag{15a}$$

$$\Delta T = 0 , \tag{15b}$$

$$w = 0 , \tag{15c}$$

while for temperature shocks Khalatnikov finds

$$\Delta T = 2(M-1)\left[\frac{\partial}{\partial T}\ln\left(\frac{a_2^3 c_p}{T}\right)\right]_0^{-1} , \tag{16a}$$

$$w = -(\rho s/\rho_n a_2)_0 \Delta T , \tag{16b}$$

$$\Delta p = -\left[\frac{\rho_s\rho_n}{\rho} - \frac{\rho^2 a_2^2}{2}\frac{\partial}{\partial p}\left(\frac{\rho_n}{\rho}\right)\right]_0 w^2 . \tag{16c}$$

Here, as in Eqs. (12) through (14), the coordinate system is shock-fixed, and the zero subscript refers to the unshocked fluid. The denominator on the right-hand side of Eq. (15a) is always positive which means that only compression shocks are to be expected in helium II. High-density regions in a propagating pressure disturbance will therefore travel faster than those of low density. However, the denominator on the right-hand side of Eq. (16a) can be either positive or negative depending on the location on the p-T diagram. On the saturated vapor pressure curve it is positive for $T < 0.5$ K and for $0.95\ \text{K} < T < 1.88$ K which means that temperature raising shocks are formed within these regions. Outside of these regions temperature lowering shocks occur.

B. Numerical solutions

Although the Khalatnikov approximations provide valuable insight into what types of shocks may be observed in helium II, they are limited to weak shocks. Furthermore, it is not clear, without examining thermodynamic data for helium II, that neglecting the coefficient of thermal expansion is consistent with this second-order approximation. Owing to the complexity of the jump conditions, for any more exact solutions one must resort to numerical methods. The numerical solutions are limited only by the quality of available thermodynamic data. We have used the data of Maynard[1] (0.3% precise), and have approximated the thermodynamic dependence on counterflow velocity to leading order in w. As discussed earlier, for the range of experimentally attainable counterflow velocities, we estimate an upper bound of 1.2% on the error introduced into our solutions by this approximation.

1. Solution method. Newton's method in three variables may be used to numerically solve the nonlinear jump conditions as follows. For a fixed upstream pressure p_0 and temperature T_0 ($w_0 = 0$ always) we seek solution vectors

$$\mathbf{x} = (p, T, w) \tag{17}$$

for the system

$$\mathbf{f}(\mathbf{x}, M) = 0, \tag{18}$$

where

$$\mathbf{f} = (f_1, f_2, f_3) \tag{19}$$

is given by Eqs. (12) through (14). The shock Mach number M is taken as the independent parameter and is referenced to either the first or second sound speed for pressure or temperature shocks, respectively. For M slightly greater than unity, the Khalatnikov approximations would be expected to give a good first guess $\mathbf{x}_0$. A better solution is then found by Newton's method (see for example, Isaacson and Keller[18]),

$$\mathbf{x}_1 = \mathbf{x}_0 - J_0^{-1}\mathbf{f}_0 . \tag{20}$$

J_0^{-1} represents the inverse of the Jacobian at the zeroth value,

$$J_0 = \left(\frac{\partial \mathbf{f}}{\partial \mathbf{x}}\right)_0 . \tag{21}$$

Iterations continue,

$$\mathbf{x}_{\nu+1} = \mathbf{x}_\nu - J_\nu^{-1}\mathbf{f}_\nu , \tag{22}$$

until each f_i approaches zero to within a specified tolerance. At higher mach numbers, the Khalatnikov solution may be such a poor guess that at best a large number of iterations are required for convergence or at worst no convergence at all is obtained. In such cases, the previous solution $\mathbf{x}^\alpha$ at Mach number M^α may be extrapolated in M and used as the initial guess $\mathbf{x}_0^{\alpha+1}$ for the current Mach number $M^{\alpha+1}$. This is effected by letting

$$\mathbf{x}_0^{\alpha+1} = \mathbf{x}^\alpha + \left(\frac{\partial \mathbf{x}}{\partial M}\right)^\alpha (M^{\alpha+1} - M^\alpha), \tag{23}$$

where

$$\left(\frac{\partial \mathbf{x}}{\partial M}\right)^\alpha = \left[\left(\frac{\partial \mathbf{f}}{\partial \mathbf{x}}\right)^\alpha\right]^{-1}\left(\frac{\partial \mathbf{f}}{\partial M}\right)^\alpha = [J^\alpha]^{-1}\left(\frac{\partial \mathbf{f}}{\partial M}\right)^\alpha . \tag{24}$$

If the solution vector $\mathbf{x}$ changes rapidly with M, the Mach number increment on the right side of Eq. (23) may be made very small to improve the quality of $\mathbf{x}_0^{\alpha+1}$.

Although it has long been known that linear "mode coupling" between first and second sound is very weak, the finite-amplitude results also show surprisingly weak nonlinear "mode coupling." The two solutions remain very distinct to high Mach numbers.

2. Implementation. Certainly one of the most crucial requirements for obtaining convergent solutions by the above method proves to be internally consistent thermodynamic data. We have used that reported by Maynard.[1] Since interpolation and numerical differentiation of the published tables provided insufficient precision to produce reliable weak wave solutions, the actual code which generated the tables (excepting chemical potential) was incorporated into the program.[19] Construction of the chemical potential by integrations with respect to pressure and temperature of Eq. (4) required the use of a lookup table of 442 reference points in order to avoid using large amounts of time required by integration from a single reference point at each iteration. Within the thermodynamic code, Maynard calculates all pressure and temperature partial derivatives using a single increment of 10^{-4} bar and 10^{-5} K, respectively. With derivatives taken on this grain, the computer-generated values for sound speeds match the experimental data points. For this reason, pressure and temperature partial derivatives within the present shock program were taken in the same way. However, since there are no corresponding natural increment sizes for counterflow velocity w or Mach number M, the analytical expressions for those partial derivatives were used.

III. RESULTS

Calculations for shock waves of both the pressure and temperature type were made for 19 different upstream states (p_0, T_0) covering the helium II p-T diagram. For each of these 38 cases, shock-induced flow states were calculated using upstream Mach number as the independent parameter. We now present a sample of the results.

A. Representative pressure shock results

Figures 3 through 9 show the results for pressure shocks with upstream state set at $T_0 = 1.80$ K and p_0 = saturated vapor pressure.

Figure 3 shows the pressure changes, $\Delta p/p_0$ versus Mach number, M for this case. The numerical solution (solid line) and Khalatnikov approximation (dashed line) coincide as they should as $M \to 1$, but for higher Mach numbers the Khalatnikov approximation underestimates the numerically calculated pressure jump. These same qualitative features in $\Delta p/p_0$ vs M are seen in the 18 other pressure shock cases as well.

Figure 4 shows the changes in temperature ($\Delta T/T_0$ vs M) for this case. While Khalatnikov approximates pressure shocks in helium II as isothermal processes, the full numerical solution (solid line) indicates a temperature decrease, the magnitude of which increases as the wave strength increases. For the strongest shock, T decreases by 0.10 K.

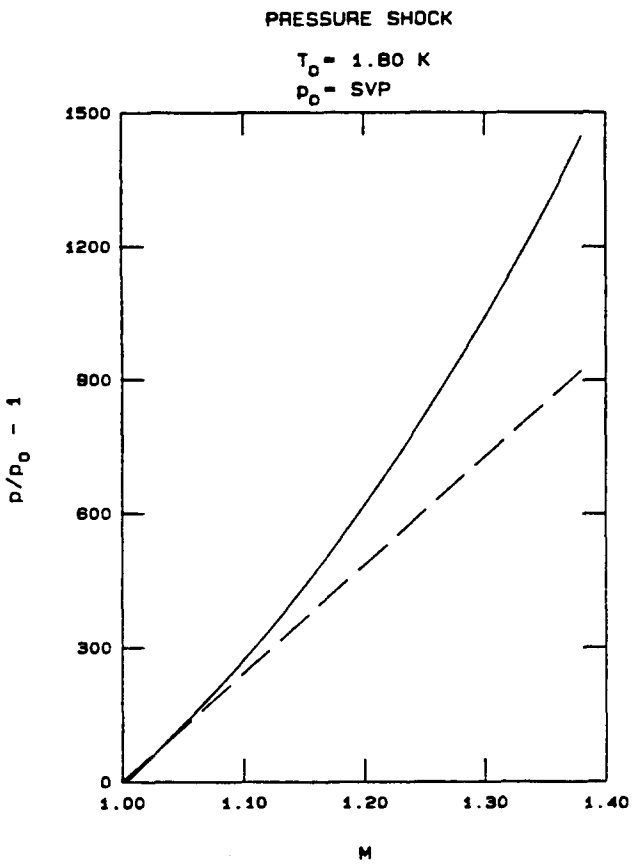

FIG. 3. Pressure jump versus upstream Mach number.

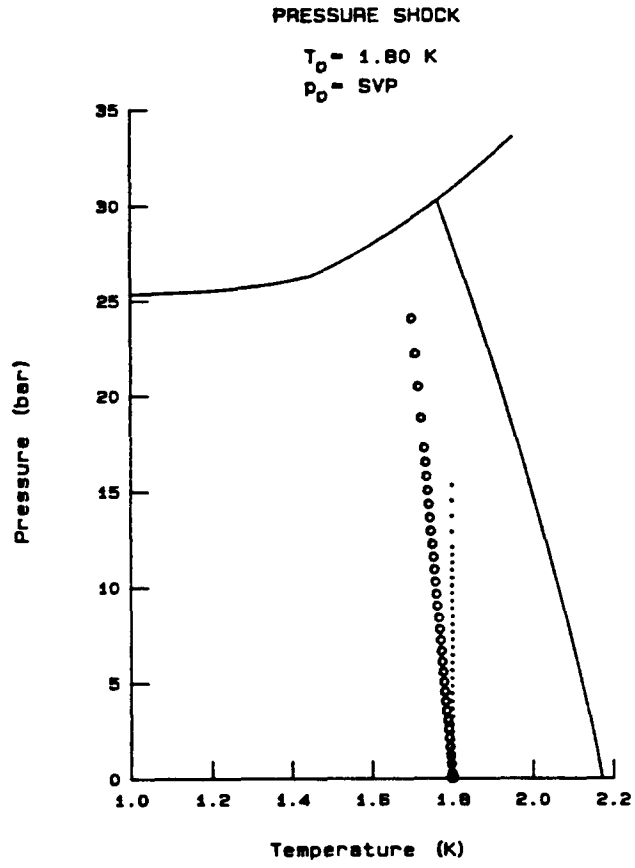

FIG. 5. Trajectories.

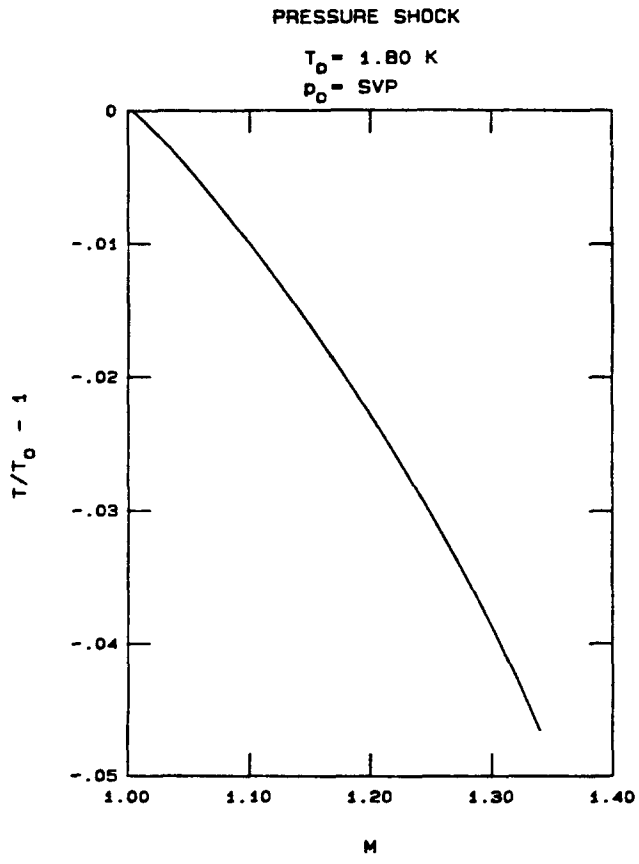

FIG. 4. Temperature jump versus upstream Mach number.

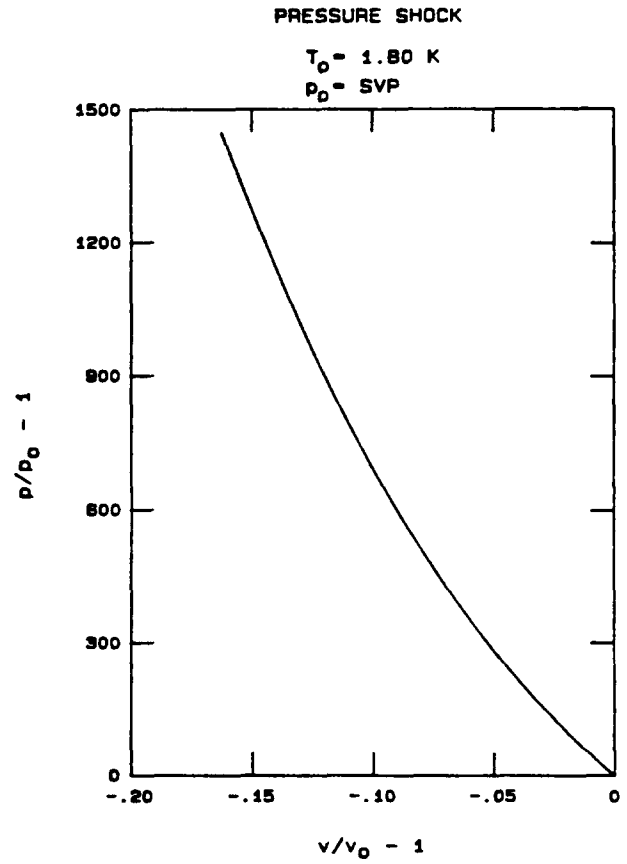

FIG. 6. Hugoniot.

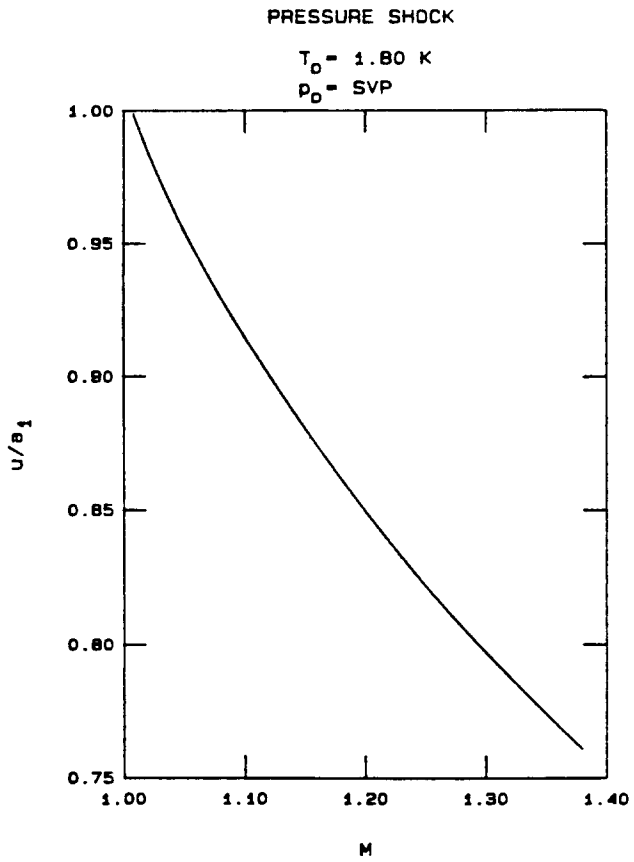

FIG. 7. Normalized downstream flow velocity versus upstream Mach number.

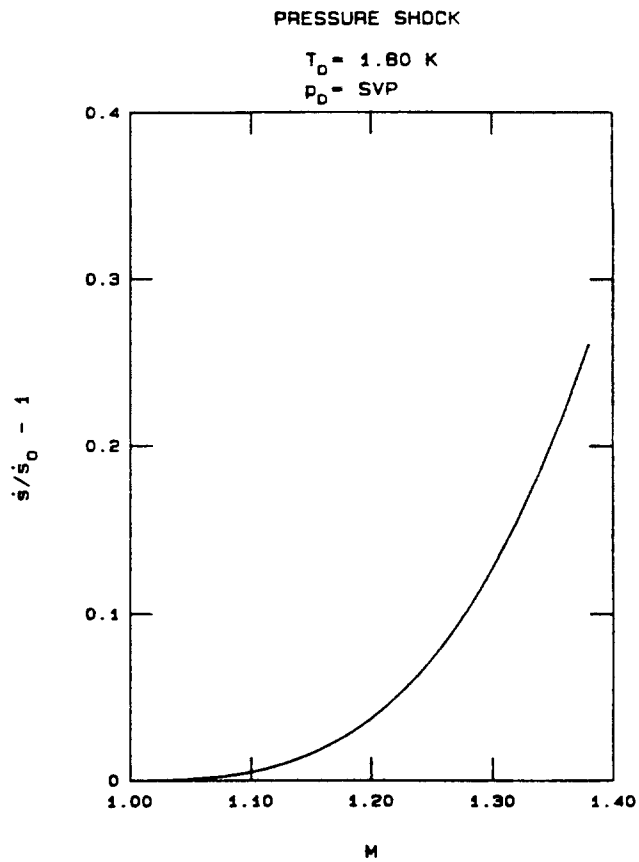

FIG. 9. Entropy flux jump versus upstream Mach number.

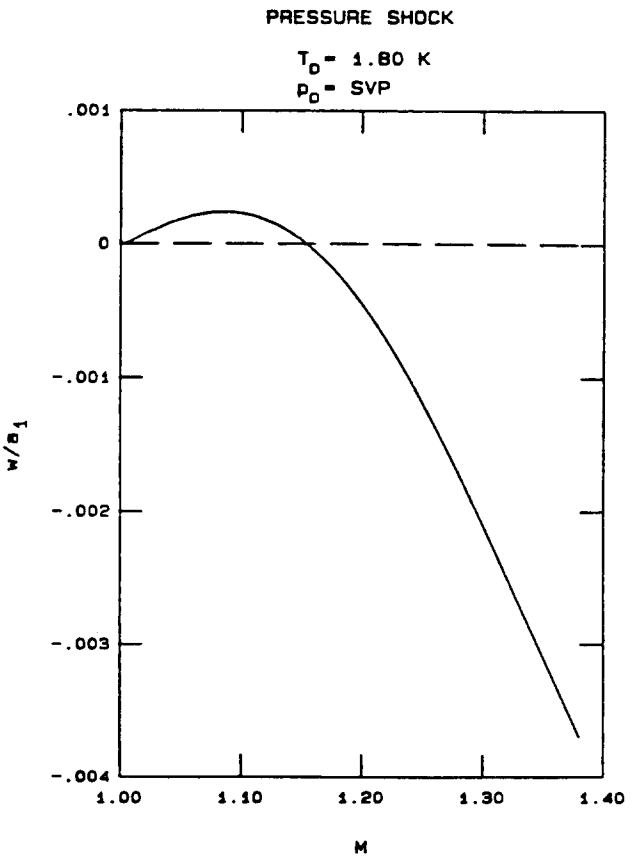

FIG. 8. Normalized downstream counterflow velocity versus upstream Mach number.

Trajectories (final states on the p-T diagram) for this case are shown in Fig. 5. The open circles are the numerical results and the dots are the Khalatnikov approximations. The highest pressure final state for the numerical solution corresponds to $M = 1.38$. Above this value, the numerical solution for downstream pressure is above 25 bar, which is very close to the melting line and outside the range of the thermodynamic data used here. Shock waves which convert liquid into solid helium are, of course, of great interest, but they are not considered here. It is also of interest to note that shock Mach numbers, which are very modest by gasdynamic standards, produce very large pressure jumps in the liquid.

The Hugoniot (locus of final states on the pressure-volume diagram) is shown in Fig. 6 and is similar to the Hugoniots seen frequently in gasdynamics. The slope is negative, as is required by the conservation laws for classical materials, while the curvature is positive, indicating occurrence of compression shocks.

Figures 7 and 8 show, respectively, the flow and counterflow velocities behind the shock normalized by the downstream first sound speed. Compression of the flow through the shock causes subsonic downstream values of u. For the counterflow velocity w produced by the pressure shock, we see an interesting behavior. Within Khalatnikov's approximations, a pressure shock induces no counterflow, but the full numerical solution (solid line) shows that in this representative case, w is initially positive (away from the shock), goes through zero at $M = 1.16$ and becomes increasingly negative (toward the shock) for higher Mach numbers. The largest magnitude of w produced is 1.3 m/sec.

In discussing entropy change across a superfluid shock wave, account must be taken of the transport of heat by convection with the normal fluid velocity. For any general fluid flow through some fixed control volume V, the second law of thermodynamics can be expressed in the form

$$\frac{d}{dt}\int_V \rho s\, dV \geqslant -\int_A \frac{\mathbf{q}}{T}\cdot d\mathbf{A}\,. \tag{25}$$

Here A is used for the closed surface bounding V, and the surface element normal vector is taken positive outward as is customary. The heat flux vector at the boundary is denoted by $\mathbf{q}$ and hence $\mathbf{q}/T$ represents the entropy flux. Since all entropy in helium II resides in the normal fluid fraction, heat flux in this liquid is given by (see Landau and Lifshitz[2])

$$\mathbf{q} = \tilde{\rho}\tilde{s}T\mathbf{u}_n\,. \tag{26}$$

Equation (25), applied to the steady, one-dimensional flow through a fixed superfluid shock, requires the downstream entropy flux to exceed that upstream. That is,

$$\dot{s} - \dot{s}_0 \equiv \tilde{\rho}\tilde{s}u_n - \rho_0 s_0 u_{n_0} \geqslant 0\,. \tag{27}$$

In a classical fluid, $u_n = u$ (since $w = 0$) and the continuity equation (8) substituted into Eq. (27) assures that the entropy itself increases across the shock. However, for superfluid shocks, the second law requires only that the entropy flux increases. Positive w corresponds to the reversible extraction of heat from the fluid behind the shock, with the consequence that the entropy itself might *decrease*.

The normalized change in entropy flux $\Delta\dot{s}/\dot{s}_0$ is shown for the representative pressure shock case in Fig. 9. Since, for pressure shocks, the counterflow velocity w is much smaller than the upstream velocity u_0, there is insignificant difference between entropy flux jump and entropy jump, and the latter is therefore not shown. Such will not be the case for temperature shocks, when $\rho_s w/\rho_0 u_0$ is large. As is deduced from very general thermodynamic reasoning, the curve for entropy flux jump has zero slope and curvature as $M\to 1$. In particular, the entropy flux change is of order $(M-1)^3$ across very weak waves.

B. Representative temperature raising shock results

As discussed previously, temperature shocks may either be temperature raising or temperature lowering processes depending on the sign of the denominator on the right side of Eq. (16a). Figures 10–15 show the calculated results for temperature shocks with upstream state set at $T_0 = 1.60$ K and $p_0 = 1.00$ bar. At this point on the p-T diagram, the above-mentioned denominator is positive, which means that temperature shocks should process this upstream state to a higher downstream temperature, at least for weak shocks.

Figure 10 shows the temperature changes, $\Delta T/T_0$ versus Mach number M for this case. As with the previously discussed pressure shock case, the numerical solution (solid line) and Khalatnikov approximation (broken line) coincide as $M\to 1$. However, for higher Mach numbers, the Khalatnikov approximation overestimates the numerically calculated temperature jump. In fact, the numerical solution for $\Delta T/T_0$ is seen to pass through a maximum of $(\Delta T/T_0)_{\max} \approx 0.07$ at $M \approx 1.50$. At Mach numbers higher than 1.50, $\Delta T/T_0$ continuously decreases. These same qualitative features for the numerically calculated temperature jumps are seen in the 13 other temperature raising shock cases as well.

Figure 11 shows the pressure jumps versus Mach number for the representative case. All strong temperature shocks in helium II, whether temperature raising or temperature lowering, are pressure-lowering processes. This is a significant effect for experiments producing strong temperature shocks in saturated liquid helium, for boiling may occur. Corresponding to the smaller magnitude of temperature increase for the numerical solution, the magnitude of the numerical pressure decrease across temperature raising shocks is also seen to be smaller than that predicted by the Khalatnikov approximation. For $M = 1.75$, the exact solution shows a pressure decrease of 0.17 bar.

Figure 12 shows the Hugoniot for this case. Remarkably, the Hugoniots for temperature raising shocks have positive slope, which for classical fluids is impossible. The reason can be seen by combining the conservation equations of mass (8) and momentum (9) to give

$$\Delta p/\Delta v = -j^2 - (v_0 + \Delta v)\rho_s\rho_n w^2/\Delta v\,, \tag{28}$$

where j is the mass flux and $v = 1/\tilde{\rho}$ is the specific volume. For classical fluids, $w = 0$, and the Hugoniot slope given by Eq. (28) is therefore always negative. For pressure shocks in helium II, $w \approx 0$, and as seen previously, $\Delta p/\Delta v$ is negative for these cases also. However, for temperature shocks, the mass flux is small, as are the jumps in pressure and density across the shock. Thus, from Eq. (28) we have

$$\Delta p/\Delta v \approx -v_0\rho_s\rho_n w^2/\Delta v\,. \tag{29}$$

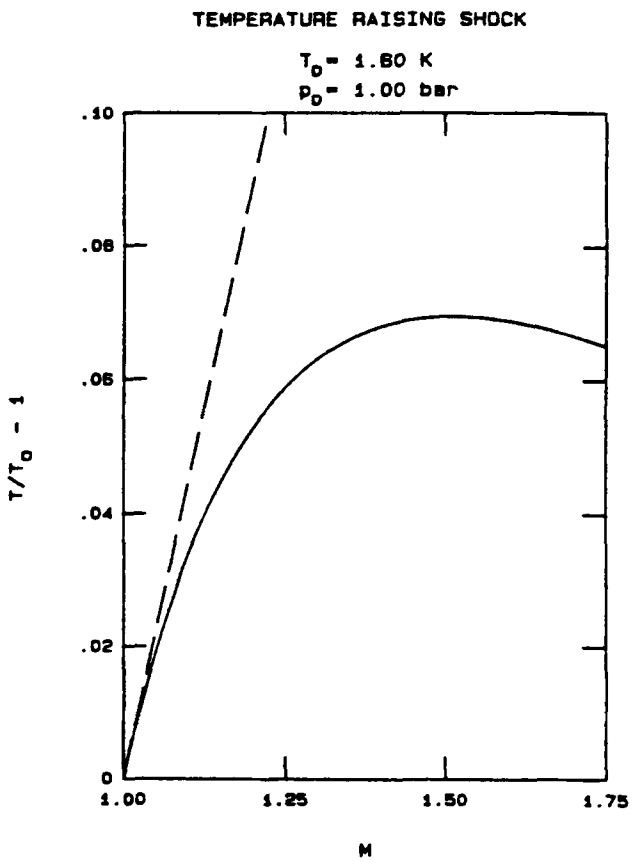

FIG. 10. Temperature jump versus upstream Mach number.

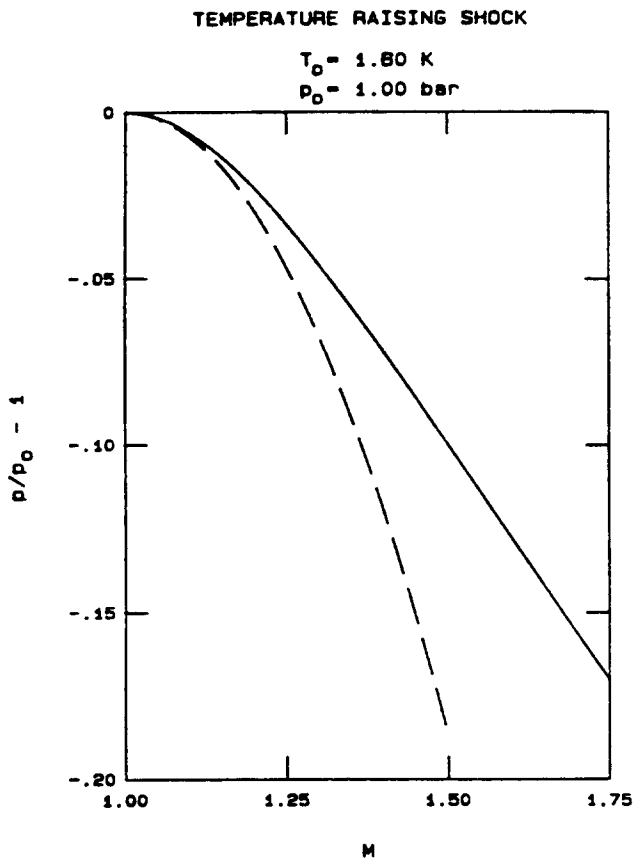

FIG. 11. Pressure jump versus upstream Mach number.

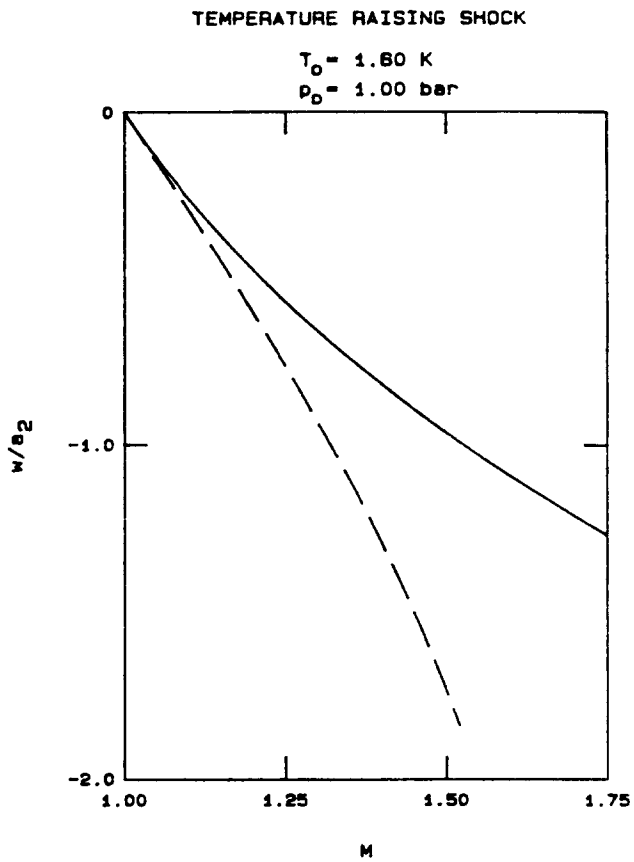

FIG. 13. Normalized downstream counterflow velocity versus upstream Mach number.

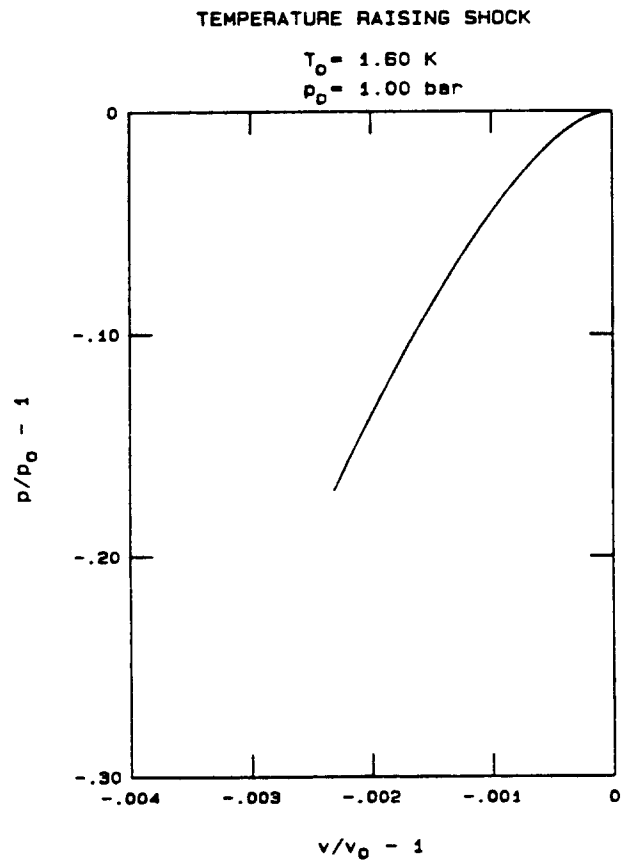

FIG. 12. Hugoniot.

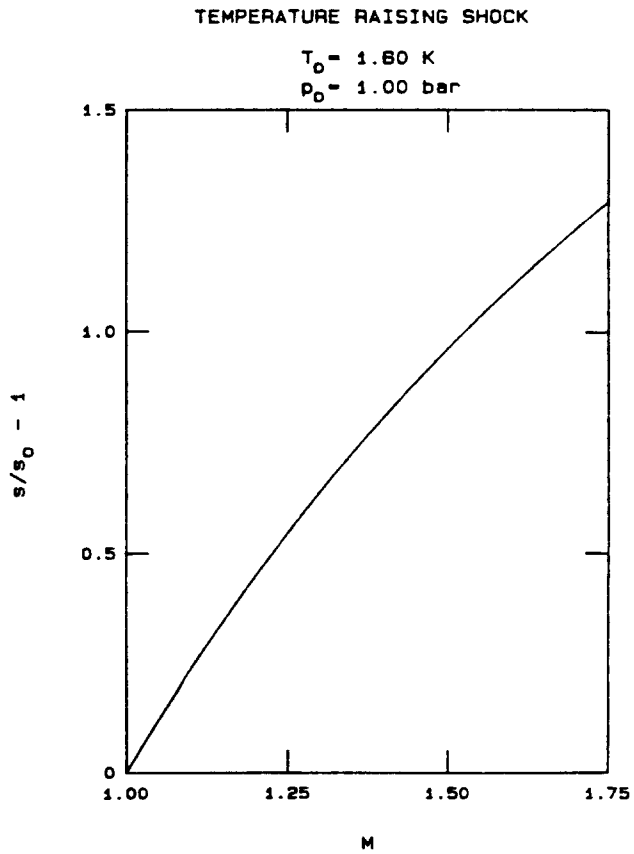

FIG. 14. Entropy jump versus upstream Mach number.

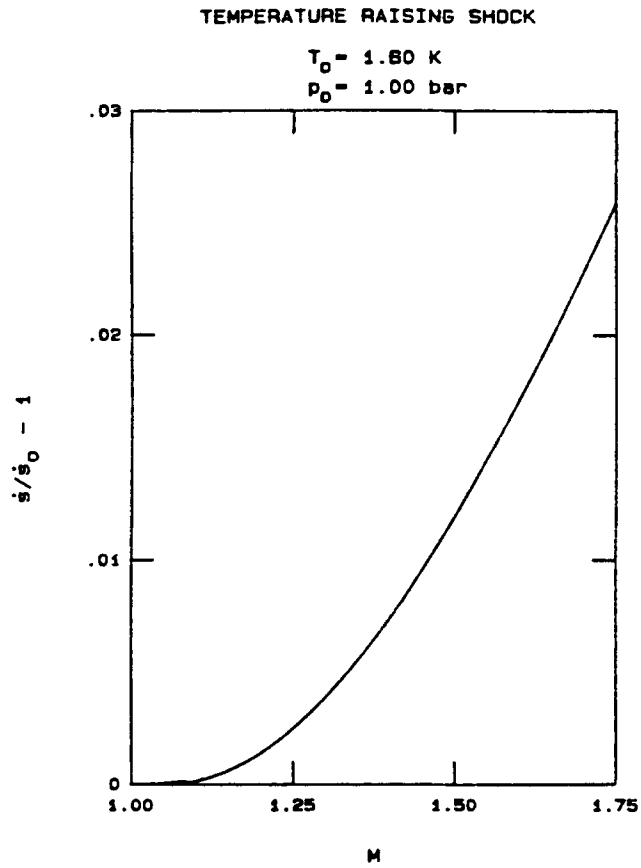

FIG. 15. Entropy flux jump versus upstream Mach number.

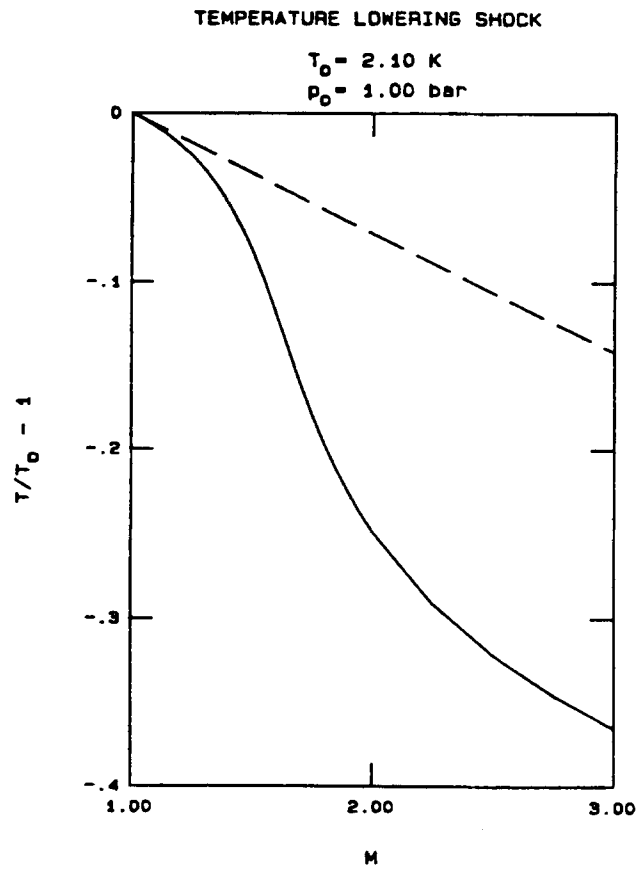

FIG. 16. Temperature jump versus upstream Mach number.

Since $\Delta p < 0$ for all temperature shocks, the sign of the Hugoniot slope is determined by the sign of Δv (change in specific volume). Since pressure changes are small, the density (i.e., inverse specific volume) change across temperature shocks is dominated by the temperature change. The negative coefficient of thermal expansion for helium II implies a specific volume decrease upon a temperature increase and vice versa. Equation (29) thus correctly predicts a positive sloping Hugoniot for temperature raising shocks and negative slopes for temperature lowering shocks.

The downstream counterflow velocity, normalized by the downstream second sound speed, is shown in Fig. 13. The sign is negative (directed toward the shock) which is an indication of heat addition from the downstream region. The counterflow velocity for a $M = 1.75$ shock wave is -25.5 m/sec. Although not shown, the jump in flow velocity, Δu, is only -0.08 m/sec for $M = 1.75$.

Plots of jumps in entropy and entropy flux for this case are shown in Figs. 14 and 15, respectively. Since the relative velocity w is large for temperature shocks, the two plots are seen to differ substantially.

C. Representative temperature lowering shock results

Figures 16 through 21 show the calculated results for temperature shocks with upstream state set at $T_0 = 2.10$ K and $p_0 = 1.00$ bar. At this point on the p-T diagram, temperature shocks are of the temperature lowering variety. It should be emphasized that all of the calculations of this paper are carried out for upstream state at rest; $w_0 = 0$. That is, only one member of the family of solutions for different up-

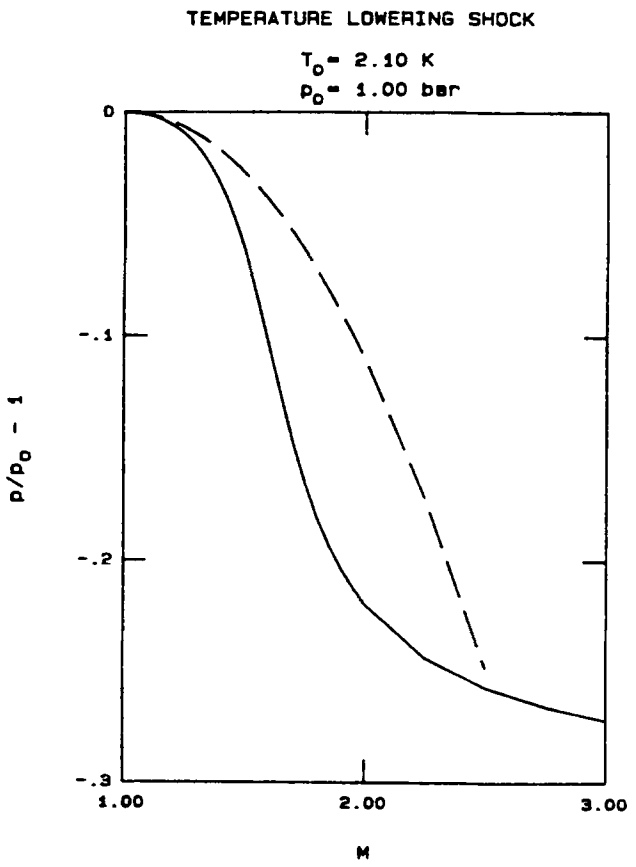

FIG. 17. Pressure jump versus upstream Mach number.

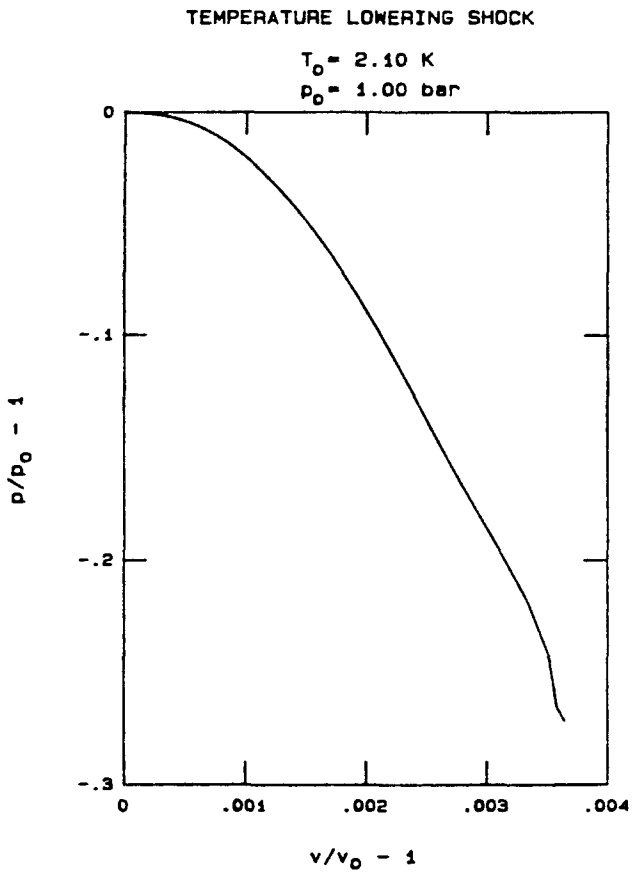

FIG. 18. Hugoniot.

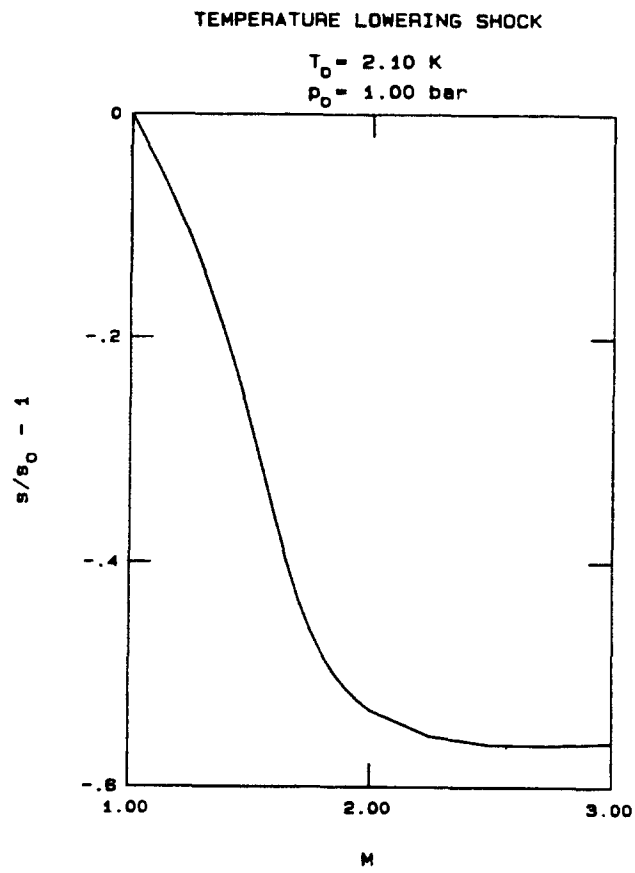

FIG. 20. Entropy jump versus upstream Mach number.

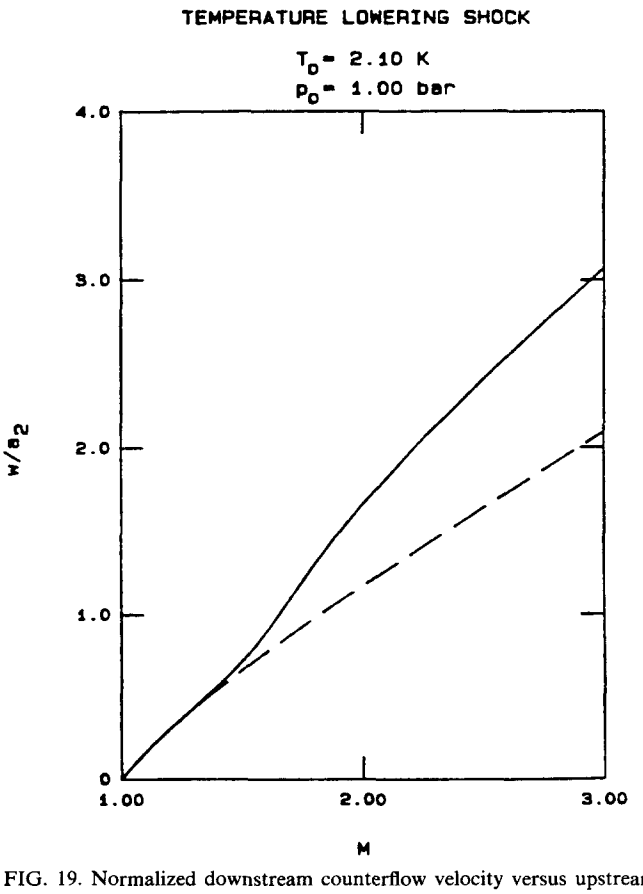

FIG. 19. Normalized downstream counterflow velocity versus upstream Mach number.

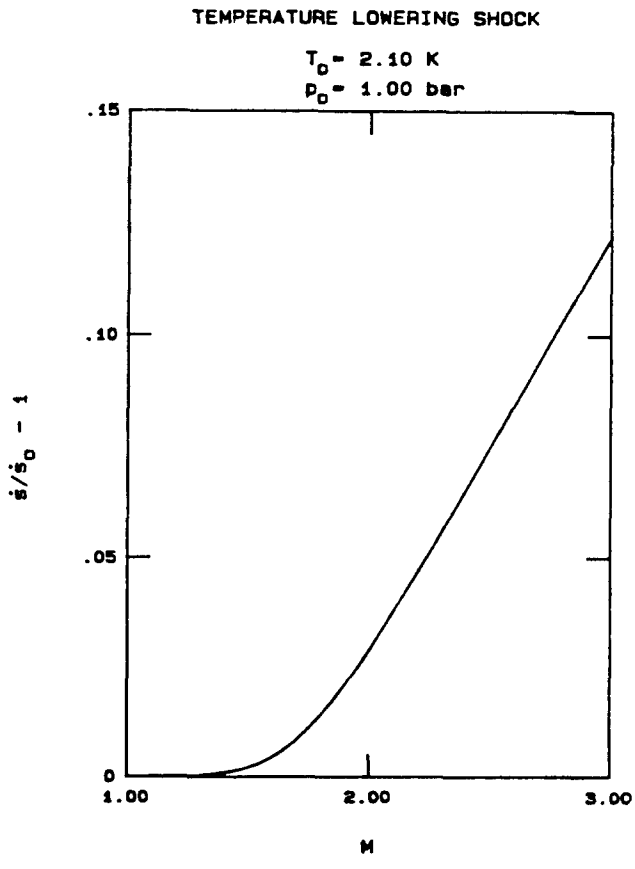

FIG. 21. Entropy flux jump versus upstream Mach number.

TABLE I. Pressure jumps across pressure shocks.

Experiment	T_0(K)	p_0	$(\Delta p/p_0)_{gas}$	$(\Delta p/p_0)_n$	$(\Delta p/p_0)_K$	M
a	1.522	SVP	1381.	1332.	1129.	1.145
b	1.665	"	602.7	558.2	489.2	1.119
c	1.751	"	642.9	583.8	479.1	1.164
d	1.832	"	446.0	498.3	400.4	1.184
e	1.989	"	293.9	244.2	208.5	1.161
f	2.031	"	298.9	202.0	176.7	1.155
g	2.095	"	315.7	283.0	226.0	1.241

stream w is presented here. On the other hand, in typical experimental setups in which temperature lowering shocks are observed, the shocks are generated by turning off a heater, in which case $w_0 \neq 0$.

From Fig. 16, it can be seen that the Khalatnikov approximation underestimates the magnitude of the temperature decrease across stronger shocks and, correspondingly from Fig. 17 the magnitude of the pressure decrease as given by Khalatnikov is also too small when compared to the exact solution. The pressure jump at $M = 1.75$ is -0.165 bar. The Hugoniot shown in Fig. 18 has a negative slope since the superfluid volume increases with decreasing temperature.

Although not shown, at $M = 1.75$, the jump in flow velocity, Δu, is approximately $+0.10$ m/sec. The counterflow velocity for a $M = 1.75$ shock wave is 24.2 m/sec, and as shown in Fig. 19, the sign of w is always positive (away from the shock) which indicates an extraction of heat from the downstream region. As a consequence of this heat extraction, the entropy change across the shock is *negative* as can be seen in Fig. 20. However, the entropy flux *increases* (see Fig. 21) as it must by the second law of thermodynamics.

D. Comparison of numerical and experimental results

Data from the experiments of Wise[12] may be compared to the numerical results for pressure shocks. In these experiments, a first sound shock in the liquid was produced by allowing a gasdynamic shock to reflect from the liquid surface. Starting at seven different temperatures T_0 on the *SVP* curve, Wise measured velocities of the incident and reflected gasdynamic shocks plus the velocity of the transmitted pressure shock in the liquid.

Using the ideal gas shock jump conditions, with the two measured wave speeds in the helium vapor, one may calculate the pressure jump on the vapor side of the interface $(\Delta p/p_0)_{gas}$. Similarly, the wave speed of the pressure shock in the liquid may be used to calculate the pressure jump on the liquid side of the interface, both numerically $(\Delta p/p_0)_n$ and by Khalatnikov's approximation $(\Delta p/p_0)_K$. The pressures across the interface should match. Table I shows these calculations with Mach number for the pressure shock in the liquid given in the right-most column.

In all seven cases, the numerical result agrees more closely than the Khalatnikov approximation to the pressure jump in the gas. For the first four cases (lower temperatures), the numerically calculated pressure jump in the liquid varies from that in the gas by 7% on the average. This represents acceptable agreement since the uncertainty in $(\Delta p/p_0)_{gas}$ is about 10%. For these same four cases, the Khalatnikov results in the liquid differ by an average of 19% from the pressure jumps in the vapor. The discrepancies for the three higher temperature cases are more serious, with the numerical and Khalatnikov results differing on average from the gas jumps by 20% and 33%, respectively.

The poorer agreement between experiment and theory for the higher temperature cases may be the result of greater evaporation rates at the liquid–vapor interface for these cases than for the lower temperature cases. As can be seen from Table II, the counterflow velocity w induced by the liquid pressure shock in the three higher temperature cases is positive, which here means toward the surface of the liquid. This also means that the initial heat flux produced is toward the surface in these cases. As a result, the tendency of the temperature raising wave [which in these cases is a fan and not a shock, since the denominator of Eq. (16a) is negative above 1.88 K] following the pressure shock into the liquid to convect heat away from the hot surface is counteracted. The evaporation rates should therefore be higher for these cases. This will tend to strengthen the reflected gasdynamic shock.

Table II compares the experimentally measured and the numerically calculated temperature jump across the transmitted pressure shocks in the liquid helium. The temperature measurements[12] were obtained with superconducting sensors in conjunction with their static calibration curves. Also shown in the right-most column are the calcu-

TABLE II. Temperature jumps across pressure shocks.

Experiment	T_0(K)	p_0	M	$(\Delta T/T_0)_{exp}$	$(\Delta T/T_0)_n$	$(w/a_{1_0})_n \times 10^4$
a	1.522	SVP	1.145	$-.0079$	$-.0117$	-11.3
b	1.665	"	1.119	$-.0126$	$-.0118$	$-.522$
c	1.751	"	1.164	$-.0200$	$-.0180$	-2.90
d	1.832	"	1.184	$-.0180$	$-.0212$	-1.99
e	1.989	"	1.161	$-.0241$	$-.0191$	4.86
f	2.031	"	1.155	$-.0291$	$-.0186$	6.07
g	2.095	"	1.241	$-.0263$	$-.0377$	8.22

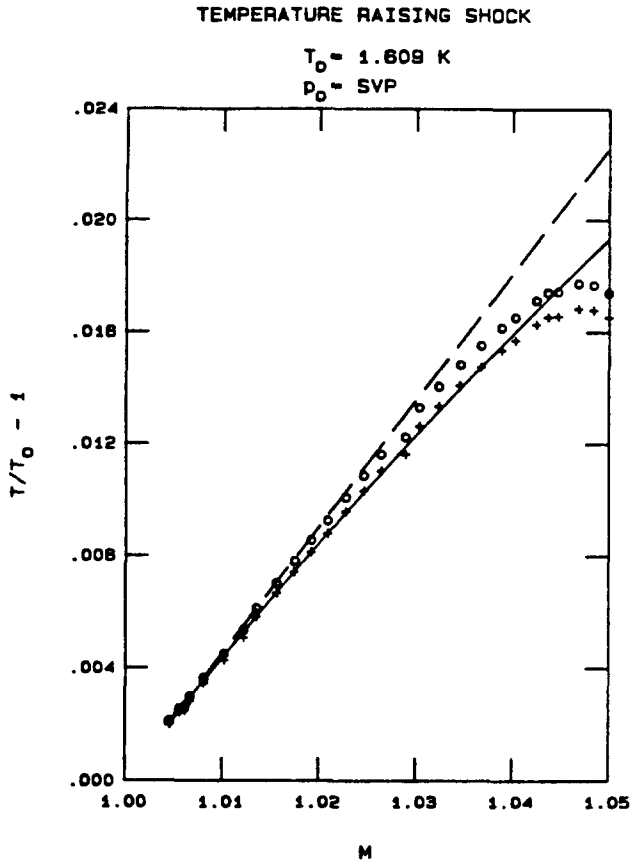

FIG. 22. Comparison to temperature shock data. Solid line is the numerical solution. Broken line is the Khalatnikov approximation. Circles are measured temperature jumps. Crosses are 95% of the measured values.

lated counterflow velocities normalized by the upstream first sound speed.

Experimental data for temperature shocks[15] may also be compared to the results from the shock program. Figure 22 shows the measured and calculated temperature jumps, $\Delta T/T_0$, as a function of temperature shock Mach number M for an initial state of $T_0 = 1.609$ K and $p_0 = SVP$. For each data point (circle), 95% of the measured value (cross) is also plotted, and it is apparent that up to $M \approx 1.04$, the numerical solution lies a constant 5% below the data. This is most likely the result of the calibration procedure used for temperature sensor measurements of the second sound shock amplitude. However, the experimental data for $1.04 < M < 1.05$ start to show significant disagreements with the numerical result. The data in this region, where the counterflow velocity w is large, may be of use in improving the thermodynamics for helium II. Specifically, the second-order approximation (5a) for the chemical potential follows from the exact differential relation (4), on the assumption that for small w, the normal fluid fraction ρ_n/ρ is approximately independent of w. Thus, with a closer analysis and better experimental data it may be possible to derive an empirical relation for the dependence of ρ_n/ρ on w. As discussed earlier, the ideal Bose theory used by Khalatnikov[4] predicts ρ_n to vary with w by less than 1.2% from its static value in these experiments, whereas Fig. 22 shows 11% disagreement between experiment and numerical result at $M = 1.05$. It might also turn out that the data from higher Mach number temperature shocks cannot be accounted for by the thermodynamics alone, and that equivalent modifications of the fundamental conservation equations are also necessary.

IV. SUMMARY

A computer program was developed to iteratively solve the shock jump conditions which follow from the Landau equations for superfluidity. The quality of thermodynamic state information used to supplement these equations allowed convergent shock solutions to be obtained for shock Mach numbers as low as 1.001 for temperature shocks and 1.004 for pressure shocks. The results asymptote to the Khalatnikov approximations for weak waves.

Pressure shocks in helium II, for the most part, exhibit the types of jumps expected in classical fluids since they produce small counterflow velocities, although $w \approx 1.3$ m/sec can be generated by strong pressure shock waves.

Temperature raising shocks show a positive sloping Hugoniot since the volume change is dominated by temperature change and not by compression.

In temperature lowering shock waves, the counterflow velocity of the shocked liquid is directed away from the shock, indicating a reversible heat extraction in the shocked region. As a consequence, the entropy *decreases* across such waves, but the entropy flux increases as it should according to the second law of thermodynamics.

Temperature shock waves can generate pressure jumps on the order of 0.2 bar and mean flow velocity jumps on the order of 0.1 m/sec.

Comparisons of the calculations to Wise's experimental data for pressure shocks reveal agreement superior to the Khalatnikov approximation in all cases. At lower temperatures the numerical results differ from the data by 7% on average. This represents acceptable agreement since the experimental precision is approximately 10%. At temperatures closer to the lambda line, where w is direct toward the liquid–vapor interface, the numerical results for Δp in the liquid are on the average 20% lower than those calculated from shock speed measurements in the vapor. This is most likely the result of evaporative effects at the liquid surface.

Comparisons of these results to the temperature shock data of Torczynski show good agreement for low Mach numbers. The data for higher Mach numbers show significant disagreement with the current two-fluid system of dynamic and thermodynamic equations. These data can possibly be used, in conjunction with exact shock wave calculations, to improve the two-fluid model.

[1] J. Maynard, Phys. Rev. B **14**, 3368 (1976).
[2] L. D. Landau and E. M. Lifshitz, *Fluid Mechanics* (Pergamon, London, 1959).
[3] S. J. Putterman, *Superfluid Hydrodynamics* (North-Holland, Amsterdam, 1974).
[4] I. M. Khalatnikov, *Introduction to the Theory of Superfluidity* (Benjamin, New York, 1965).

[5]R. J. Atkin and N. Fox, J. Phys. C. **16**, 1615 (1983).
[6]I. M. Khalatnikov, Zh. Eksp. Theor. Fiz. **23**, 253 (1952).
[7]As is well known, in classical fluids irrotationality is preserved across plane shock waves. Downstream vorticity is produced from a uniform upstream state only by shocks of nonuniform strength, e.g., curved shocks.
[8]D. V. Osborne, Proc. R. Phys. Soc. London Ser A. **64**, 114 (1951).
[9]A. J. Dessler and W. M. Fairbank, Phys. Rev. **104**, 6 (1956).
[10]J. C. Cummings, Ph.D. thesis, California Institute of Technology, 1973.
[11]J. C. Cummings, D. W. Schmidt, and W. J. Wagner, Phys. Fluids **21**, 713 (1978).
[12]J. L. Wise, Ph.D. thesis, California Institute of Technology, 1979.
[13]T. N. Turner, Ph.D. thesis, California Institute of Technology, 1979.
[14]T. N. Turner, Physica **107B**, 701 (1981).
[15]J. R. Torczynski, Ph.D. thesis, California Institute of Technology, 1983.
[16]B. Sturtevant, Bull. Am. Phys. Soc. **21**, 1223 (1976).
[17]H. Kojima, W. Veith, E. Guyon, and I. Rudnick, J. Low Temp. Phys. **25**, 195 (1976).
[18]E. Isaacson and H. B. Keller, *Analysis of Numerical Methods* (Wiley, New York, 1966).
[19]S. Baker (private communication).